THE JOURNAL OF PHYSICAL CHEMISTRY B

ARTICLE

pubs.acs.org/JPCB

Using Symmetry Breaking for Directed Transport of Paramagnetic Colloids on Garnet Films

S. Aliaskarisohi,[†] T. H. Johansen,[‡] and Th. M. Fischer*[,†]

[†]Institut für Experimentalphysik, Universität Bayreuth, 95440 Bayreuth, Germany

[‡]Department of Physics, University of Oslo, P.O. Box 1048, Blindern, 0316 Oslo, Norway

ABSTRACT: The transport behavior of paramagnetic particles on top of a ferrimagnetic garnet film is investigated in a modulated external magnetic field. Broken symmetries are required to direct the transport of the particles. We provide such symmetry breaking by tilting the external field modulation with respect to the normal direction of the garnet film and by the intrinsic geometrical symmetry breaking of the garnet film magnetic pattern. The interplay of both symmetry breaking mechanisms causes a rich variety in transport behavior and direction. We corroborate our experimental transport directions by comparing experimental with theoretical transport phase diagrams. Directing the transport of paramagnetic colloids will be useful when they are loaded with biomedical cargo on a magnetic lab-on-a-chip device.

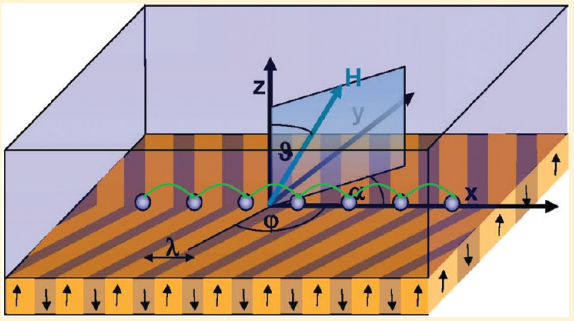

1. INTRODUCTION

Deterministic[1,2] as well as statistical ratchets[3−5] convert the bounded periodic or stochastic dynamics of an external field into the driven unbounded motion of objects coupling to the external force. A wheel exerts a continuous thrust to the ground it moves on. A ratchet in contrast exerts a thrust only during a critical period of time when the moving object experiences instability in the energy landscape generated by the external force. A broken symmetry during this instability is necessary to direct the thrust in the desired direction. The motion of the object is a sequence of hops during the instability and periods where the particle is largely arrested in a local minimum of the energy landscape.

Here we are interested in the transport direction of paramagnetic colloidal particles on a magnetic garnet film[6] when having two competing ways of breaking the symmetry of a magnetic stripe pattern. Either the symmetry is broken by tilting the external magnetic field with respect to the film normal or a wedge geometry of the stripes imposes a preference direction. Both ways to break the symmetry span a 2D parameter space, where different directions of motion are possible. The responses in motion of the particles to the two ways of breaking the symmetry are correlated: When both symmetry breaking mechanisms are used simultaneously, they may lead to a transport directions opposite to either way used individually.

2. EXPERIMENT

We experimentally observe the transport of paramagnetic colloids on a magnetic garnet film when driven with an external magnetic field. A scheme of the experiment is shown in Figure 1.

We studied the hopping of paramagnetic colloids (Dynabeads-M-270 carboxylic acid) with a diameter of $2a = 2.8 \pm 0.1\ \mu$m, effective susceptibility $\chi_{\text{eff}} = 0.17$, and concentration of 2×10^9 beads/mL purchased from Invitrogen. The original particle solution is diluted with pure water (Millipore milli-Q water 18.2 MΩ × cm) to a concentration of 2×10^7 beads/mL and placed on two different 4 μm thick magnetic garnet films of composition $Y_{2.5}Bi_{0.5}Fe_{5-q}Ga_qO_{12}$, which were epitaxially grown on a gadolinium gallium garnet substrate. The resulting ferrimagnetic films have a uniaxial anisotropy with a spontaneous magnetization of $M_s = 8.4$ and 9.2 kA/m. Magnetic stripe domains are magnetized perpendicular to the film and alternate between up and down magnetization with average wavelength of $\lambda = 12$ and 14 μm, respectively. The persistence length of the garnet films used is limited, and the stripes abruptly change direction, creating wedges in the pattern that are characterized by the angle φ between one arm of the stripe pattern and the wedge bisector. The angle φ is one of the symmetry breaking parameters that can induce directed motion. In our films, there is a distribution of wedge angles in the range of $45 < \varphi < 120°$. The garnet films were coated with polysodium 4-styrene sulfonate to prevent adhesion of particles to the surface.

An external time-dependent magnetic field $\mathbf{H}_{\text{ext}}(t) = \mathbf{H}^0_{\text{ext}} e^{i\omega t}$ drives the motion of the particles with a frequency of $\omega/2\pi = 5$ Hz. The orientation of the field $\mathbf{H}^0_{\text{ext}} = H_{\text{ext}}$ (cos α sin ϑ, sinα sinϑ, cosϑ) with respect to the film and the wedge is characterized by the tilt angle $\vartheta = 23°$, which serves as an additional

Received: December 14, 2010
Revised: January 25, 2011
Published: February 22, 2011

symmetry breaking parameter directing the motion of the particles. It is produced by two solenoids oriented perpendicular and parallel to the film. The orientation α of the wedge bisectors to the magnetic field is randomly distributed allowing the full range $0 < \alpha < 2\pi$ to be probed. The amplitude of the magnetic field was set to $H_{ext} = 0.165 \times 10^4$ A/m.

Polarization microscopy was used to visualize simultaneously the domain pattern and the particle transport. Domains are visible because of the polar Faraday effect. Movies of the particle transport were recorded, digitized using a digital camera (A311 fc BASLER), and stored on a computer for further analysis.

3. TRANSPORT INSTABILITY

The superposition of the heterogeneous magnetic field produced by the garnet film pattern and the homogeneous external time-dependent field results in a magnetic field that varies in both space and time. The normal component of the external field additionally affects the position of the domain walls because the normal field increases the width of the domains having a magnetization parallel to the field and decreases the width of the antiparallel ones. As a result, the positions $x_{\pm}^{m} = \lambda/4[(4m + 1) \pm (1 + H_{ext}/M_s \cos \vartheta \sin(\omega t))]$, $m = 0, 1, 2, ...$, where the domain walls intersect the bisector of the wedge, also oscillate as a function of time. The external magnetic field therefore both superposes to and perturbs the magnetic field of the garnet film. The paramagnetic particles of volume $V = 4\pi a^3/3$ above the garnet film experience the total magnetic field, where they have a magnetic energy of $E = -V\mu_0\chi_{eff}H^2$. Here μ_0 denotes the vacuum permeability. In the absence of an external field, this energy is minimized above the intersection of the domain walls with the wedge bisector, and the particles are localized at those positions. The minimal position may be computed from the condition $\nabla E = 0$. A weak external field slightly perturbs the energy of the particles; however, the energy minima remain stable at all times and move in a bounded region around the zero-external field position. The result is a particle motion that is bounded and locked to the motion of the domain wall position. A sketch of such bounded particle motion is depicted in Figure 2a. The particles return to their original position after one period of the modulation, and no net motion of the particle results from the modulation.

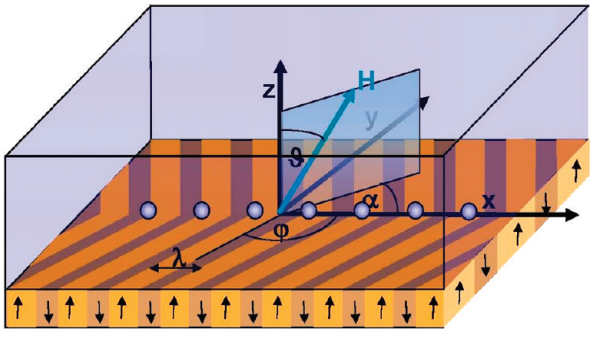

Figure 1. Scheme of a magnetic garnet film with alternating magnetized wedge domains, the paramagnetic particles in aqueous solution placed above the film. The film is modulated with a tilted oscillating external magnetic field. Particles will transport along the wedge bisector of angle φ. The transport direction depends on the angle between wedge bisector and in-plane field, α, and the tilt angle of external field, ϑ.

The situation changes when the external field surmount a critical threshold $H_{ext} > H_c$. At the critical field, the energy minimum converts to a saddle point $(\xi \cdot \nabla)^2 E = 0$, and the particle hops into an adjacent minimum along the unstable direction defined by the vector ξ. If the energy landscape happens to be symmetric, then the particle has the choice to hop in either positive $(+\xi)$ or the negative $(-\xi)$ direction, and the resulting motion is a stochastic hopping resulting in a diffusive dispersion of the particles. A sketch of such stochastic hopping is depicted in Figure 2b. The motion is unbounded, but no net direction of the motion results from this form of modulation.

Directed motion may result when the symmetry is broken, whereas the external field reaches the critical threshold H_c. For that situation, the minimum converts to a true saddle point $(\xi \cdot \nabla)^3 E \neq 0$, and the particle has only one choice of direction to hop to the next minimum. A smart way of external modulation will lead to a consecutive sequence of instabilities where the particle-carrying minimum is converted to a saddle point that directs the particle always in the same direction. Figure 2c shows the directed motion of such a smart modulation.

In the work of Tierno et al.,[78] all three kinds of hopping have been explained for a garnet film with stripe pattern, and paramagnetic particles were placed above it. They showed that tilting

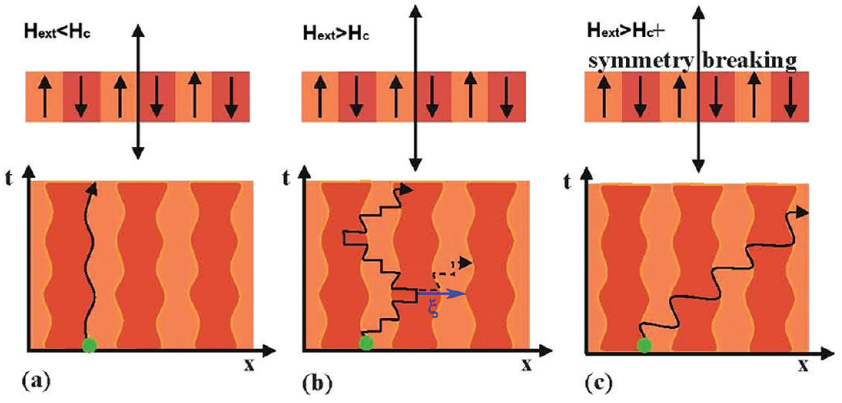

Figure 2. Sketch of the possible forms of motion above the modulated magnetic garnet film pattern. (a) In a weak external field $H_{ext} < H_c$, particles are locked to the motion of the domain walls. (b) In an external field normal ($\vartheta = 0$) to a straight $\varphi = \pi/2$ stripe pattern surmounting the critical field $H_{ext} > H_c$, the domain wall positions become unstable, resulting in a diffusive hopping with no net direction of the transport. (c) Breaking the symmetry by tilting the field ($\vartheta = 0$) or using a wedge $\varphi = \pi/2$ causes a smart sequence of instabilities that let the particles hop always into the same direction as their pervious steps.

dx.doi.org/10.1021/jp1118585 |J. Phys. Chem. B 2011, 115, 2243–2247

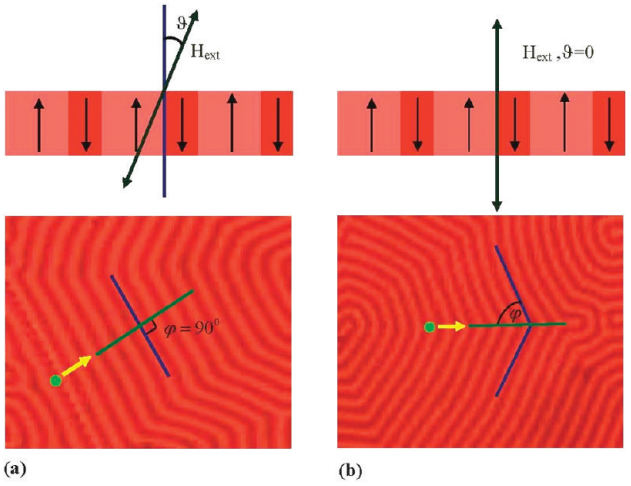

Figure 3. Two ways of breaking the symmetry: (a) By applying the external tilted field, the particles hop perpendicular to the stripes in the direction of the tilt. (b) With a wedge pattern, one forces the particles to hop along the bisector against the direction of the curvature.

the modulated field with respect to the film normal ($\vartheta \neq 0$) represents a smart way to direct the particles into one direction. Another form of smart modulation was discovered by Dhar et al.,[9] who used the stripe curvature to direct ferrofluid-filled mouse macrophages.

The current work aims at experimentally and theoretically studying the effect of combining different ways of smart modulation. Here we break the symmetry by either tilting the field with respect to the film or by using wedge patterns to direct the particles. As will be shown, the resulting motion of the particles is more complex than what one would guess from the results of the individual ways to break the symmetry.

4. EXPERIMENTAL RESULTS

Figure 3 shows the hopping direction for the two different ways to break the symmetry. The particles above a straight stripe pattern hop in the direction of the tilt, whereas the particles above the wedge pattern in an external field normal to the film are directed along the wedge bisector against the direction of the curvature of the wedges.

The situation is much more complex when we apply both ways to break the symmetry. Figure 4 shows the hopping direction of different wedges on the same garnet film when subject to a field that is tilted with respect to the film normal. The wedges have different values of both the wedge angle φ and the bisector orientation α. In contrast with the situation when the external field is oriented normal to the film, hopping directions both against and along the wedge curvature are observed.

Although the behavior is much more complex when both symmetry breaking mechanisms are present, the transport remains smart with a definite direction of the hopping. The direction of the hopping is a result of the magnetic energy landscape at the time of the instability. It depends on the three parameters ϑ, φ, and α. We have experimentally determined the phase diagram of the hopping directions as a function of two of those parameters. Before presenting those results in Section 6, we give a theoretical description of the energy landscape.

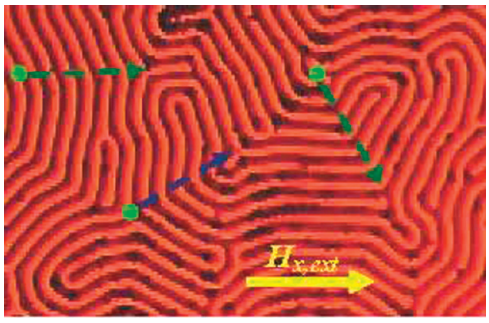

Figure 4. Transport directions above a stripe-patterned film in a tilted magnetic field with wedges. The tilt direction is along the x axis. Particles are transported along the bisectors of the wedges either in direction (blue) or against (green) the direction of the curvature of the wedge.

5. ENERGY LANDSCAPE OF A WEDGE PATTERN

The magnetic field above the garnet film fulfills the magnetostatic form of Maxwell's equations

$$\nabla \cdot \mathbf{H} = 0 \tag{1}$$

and

$$\nabla \times \mathbf{H} = 0 \tag{2}$$

with the boundary conditions

$$H_z(x, y, z = 0^+) = M_z(x, y, z = 0^-) = \pm M_s \tag{3}$$

at the garnet film/water interface and

$$\mathbf{H}(z \to \infty) = \mathbf{H}_{ext} \tag{4}$$

far from the interface. Equation 2 may be expressed in scalar form using the magnetostatic potential ψ satisfying $\mathbf{H} = \nabla\psi$. The magnetostatic potential fulfills the Laplace equation $\nabla^2\psi = 0$, and its solution[10] subject to the above boundary condition reads

$$\psi = \mathrm{H}_{ext} \cdot x - (M_s + H_{z,ext})(\psi_{N,+} - \psi_{-N,-}) + 2M_s \sum_{n=-N}^{N} (\psi_{n,+} - \psi_{n,-}) \tag{5}$$

where

$$\psi_{n,\pm} = \frac{1}{2\pi}[2z \operatorname{arccot} \frac{x - x_{n,\pm} + r_{n,\pm} \cos\varphi}{z \sin\varphi} + 2y \cos\varphi \operatorname{atanh} \frac{y \sin\varphi}{r_{n,\pm} + (x - x_{n,\pm}) \cos\varphi} - x \sin\varphi \ln((r_{n,\pm}^2 - z^2)\cos^2\varphi + 2r_{n,\pm}(x - x_{n,\pm}) \cos\varphi + r_{n,\pm}^2 - y^2)] \tag{6}$$

where $r_{n,\pm}^2 = (x - x_{n,\pm})^2 + y^2 + z^2$ and where N cuts off the number of stripes at the wedge.

By knowing the field, we can compute the magnetostatic energy landscape of the paramagnetic particles. A contour plot of this landscape at the elevation $z = a = 0.07\lambda$ is shown in Figure 5 along the bisector coordinate x as a function of time t. In this particular example ($\varphi = 60°$, $\alpha = 45°$, $\vartheta = 23°$, and $H_{ext} =$

dx.doi.org/10.1021/jp1118585 |J. Phys. Chem. B 2011, 115, 2243–2247

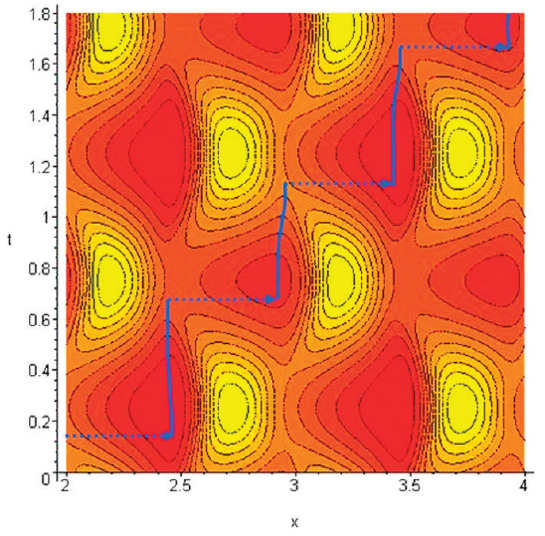

Figure 5. Contour plot of the magnetostatic potential as a function of the bisector coordinate x and the time t. The red regions correspond to the minima, and the yellow regions are maxima of the potential. The trajectory of one particle is depicted in blue.

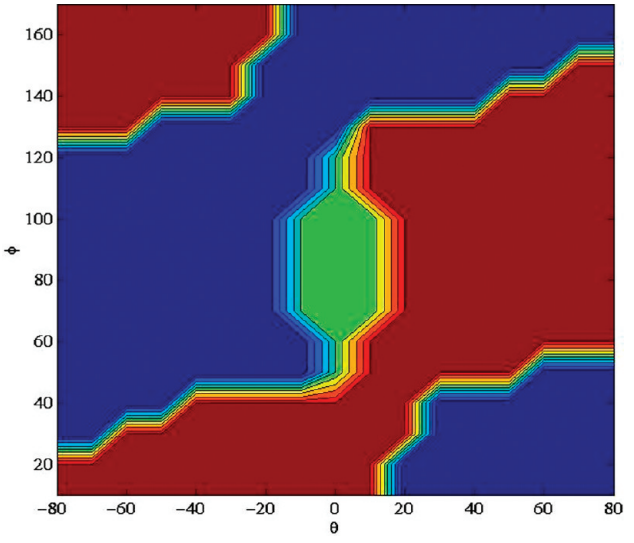

Figure 6. Theoretical phase diagram of the transport behavior of wedges with bisectors oriented into the tilt direction of the magnetic field ($\alpha = 0$) as a function of the tilt angle ϑ and the wedge angle φ. The green region corresponds to a locked phase without particle transport. The red and blue phases are phases where particles hop toward the right and the left, respectively.

$0.25M_s$), the potential minima merge with maxima to the right, creating a saddle point at $x = (0.5 + n)\lambda$ at the time $\omega t = 0.6$ that lets the particle hop to the right. A trajectory of a particle will follow the blue line in Figure 5. Hence, the contour plots allow us to read off the direction of the hopping for a particular set of parameters.

6. TRANSPORT PHASE DIAGRAMS

Shown in Figure 6 is the phase diagram of hopping of the particles in terms of the wedge angle φ and the tilt angle ϑ. The tilt direction of external field for this phase diagram coincides

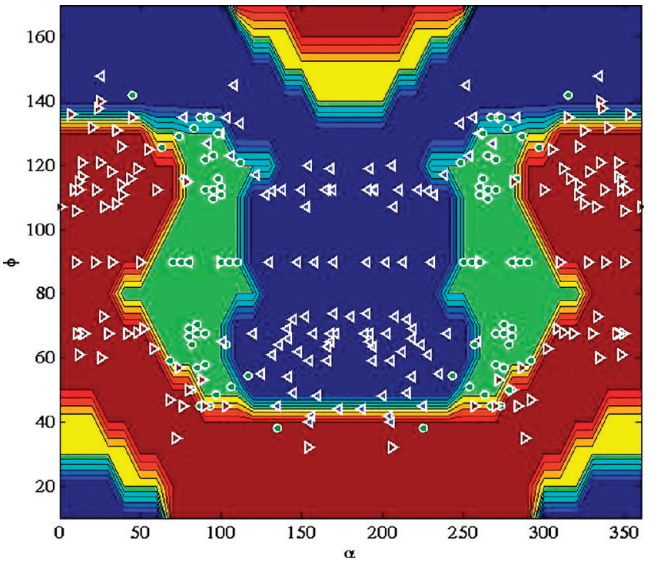

Figure 7. Theoretical and experimental phase diagram of the transport behavior of wedges with a tilt of the field of $\vartheta = 23°$ as a function of the bisector orientation α and the wedge angle φ. The green regions correspond to a locked phase without particle transport. The red and blue phases are phases where particles hop toward the right and the left, respectively. In the yellow phase, the simultaneous symmetry breaking mechanisms do not result in a smart modulation, and particles hop either way. Experimental data points (○, no hopping; left-pointing triangle, hopping toward the left; and right-pointing triangle, hopping toward the right).

with the bisector of the wedge ($\alpha = 0$). We find three different phases marked in red, blue, and green. In the green phase, the tilt and the deviation of the wedge angle from a straight stripe are insufficient to cause directed motion of the particles. It corresponds to a localized phase where the particles are locked to the domain walls. The red and blue phases, in contrast, are phases where the particles are directed toward the right and the left, respectively, and in this phase diagram, the field projection for $\vartheta > 0$ is toward the right, and for $\vartheta < 0$, it is toward the left. For $\varphi = 90°$, the wedge degenerates to a straight stripe pattern, and the hopping direction is determined by the tilt angle. The direction of the hopping remains tilt-dominated for a broad region $\varphi = 90 \pm 35°$ around the straight stripes. Only for sharp wedge angles $\varphi < 45°$ and $\varphi > 125°$ can the angle of the wedge reverse the behavior dictated by the tilt. If we concentrate on these regions and focus on the behavior in the absence of tilt $\vartheta = 0$, then we conclude that the wedge breaks the symmetry in a way so as to support hopping against the direction of the wedge curvature. One would guess that this should be in synergy with the situation encountered when the tilt is also pointing against the curvature of the wedge. In the phase diagram of Figure 6, however, we find the region $\varphi < 45°$ and $\vartheta > 25°$, where the particle hop is in direction of the curvature and opposite to the tilt direction. This shows that a simple superposition principle does not hold for nonlinear processes, and the resulting hopping direction is opposite to what would be expected if one applies both symmetry breaking mechanisms individually.

In the experiments, we kept the tilt angle fixed at $\vartheta = 23°$. The wedge angle φ and the bisector orientation to the external field α, however, varied because of the distribution of wedge angles and bisector orientations on the film. In Figure 7, we plot the transport phase diagram as a function of the latter angles and

incorporate the experimental measurements. We use the same color coding as in Figure 6. The additional color yellow corresponds to a region where the combination of the two symmetry breaking effects does not result in a smart modulation, and one finds particles hopping to the right and to the left simultaneously.

In Figure 7, for wedge angles φ ranging from 45 to 125°, we are in the tilt-dominated regime, and the hopping in this region usually follows the direction dictated by field. Only when $\alpha \approx 90$ or 270° does the component of the tilt along the bisector become too weak to cause directed motion, and the particles fall into the locked localized phase. In the wedge-dominated regime $\varphi < 45°$ and $\varphi > 125°$, the hopping is into the direction against the wedge curvature if the tilt angle also does not point in this direction. When the tilt points against the direction of the wedge curvature (blue regions in the lower corners and red region at the upper boundary of Figure 7), the particles hop in the direction of the curvature and against the tilt direction. This corresponds to the region also found in Figure 6, where the particles hop opposite to the direction encountered when both symmetry breaking mechanisms are applied individually

The experimental data points that are inserted in Figure 7 confirm the theoretical predictions. Most of the data lie in the region $40 < \varphi < 140°$ and agree with the theoretical phase diagram. Data points that disagree with the theory are located in the vicinity of the theoretical phase boundaries. Our data confirm the changes of hopping directions in the tilt-dominated regions $45 < \phi < 120°$ as well as the transition to the wedge-dominated phases. So far we could not prove or disprove the existence of phases where particles are predicted to hop into the opposite direction than with the symmetry breaking mechanisms applied individually. We also could not experimentally confirm the loss of smart modulation in the yellow regions. The experimental access to these regions would require wedges with opening angles $\varphi <$ 45°, which were not available in the present samples.

7. CONCLUSIONS

The directed transport of paramagnetic colloidal particles placed above a magnetic garnet film requires a symmetry breaking mechanism. Such symmetry breaking mechanism can be achieved by applying a modulated tilted external magnetic field or by an intrinsic symmetry breaking wedge pattern in the film. When both symmetry breaking mechanisms are applied simultaneously, complex transport behavior results that does not necessarily reflect the transport behavior of the particles when each mechanism is used individually. Theoretically deduced phase diagrams correspond well with the experimentally determined phase diagrams. Our findings might be useful for the transport of biomedical cargo with paramagnetic particles on a lab-on-a-chip device.

AUTHOR INFORMATION

Corresponding Author

*E-mail: thomas.fischer@uni-bayreuth.de.

ACKNOWLEDGMENT

This work has been supported by the German Science Foundation within the Center of Excellence SFB 840 and the Norwegian Research Council.

REFERENCES

(1) Dialynas, T. E.; Lindenberg, K.; Tsironis, G. P. *Phys. Rev. E* **1997**, *56*, 3976.
(2) Mateos, J. L. *Phys. Rev. Lett.* **2000**, *84*, 258.
(3) Lehmann, J.; Reimann, P.; Hänggi, P. *Phys. Rev. Lett.* **2000**, *84*, 1639.
(4) Reimann, P.; Hänggi, P. *Appl. Phys. A: Mater. Sci. Process.* **2002**, *75*, 169.
(5) Hastings, M. B.; Reichhardt, C. J. O.; Reichhardt, C. *Phys. Rev. Lett.* **2003**, *90*, 247004.
(6) Tierno, P.; Sagues, F.; Johansen, T. H.; Fischer, T. M. *Phys. Chem. Chem. Phys.* **2009**, *11*, 9615.
(7) Tierno, P.; Reddy, V. S.; Roper, M. G.; Johansen, T. H.; Fischer, T. M. *Phys. Rev. E* **2007**, *75*, 041404.
(8) Tierno, P.; Reddy, V. S.; Johansen, T. H.; Fischer, T. M. *J. Phys. Chem. B* **2008**, *112*, 3833.
(9) Dhar, P.; Tierno, P.; Johansen, T. H.; Fischer, T. M. *J. Phys. Chem. B* **2007**, *111*, 13097.
(10) Morse, P. M.; Feshbach, H. *Methods of Theoretical Physics Part II*; McGraw Hill: New York, 1953.